



Article

Copper Chloro-Complexes Concentrated Solutions: An Electrochemical Study

Giampaolo Lacarbonara ¹, Luigi Faggiano ¹, Stefania Porcu ², Pier Carlo Ricci ², Stefania Rapino ¹, Declan P. Casey ³, James F. Rohan ³ and Catia Arbizzani ^{1,*}

¹ Department of Chemistry “Giacomo Ciamician”, Alma Mater Studiorum-University of Bologna, Via F. Selmi 2, 40126 Bologna, Italy; giampaol.lacarbonar2@unibo.it (G.L.); luigi.faggiano3@unibo.it (L.F.); stefania.rapino3@unibo.it (S.R.)

² Department of Physics, University of Cagliari, SP 8 Km 0.700, 09042 Cagliari, Italy; stefania.porcu@unica.it (S.P.); carlo.ricci@unica.it (P.C.R.)

³ Tyndall National Institute, Lee Maltings, University College Cork, T12R5CP Cork, Ireland; declan.casey@tyndall.ie (D.P.C.); james.rohan@tyndall.ie (J.F.R.)

* Correspondence: catia.arbizzani@unibo.it

Abstract: Basic studies on concentrated solutions are becoming more and more important due to the practical industrial and geological applications. The use in redox flow batteries is one of the most important applications of these solutions. Specifically, in this paper we investigated high-concentrated copper chloro-complexes solutions with different additives. The concentration of ligands and additives affects the physicochemical and electrochemical properties of 2 M solutions of Cu(I) and Cu(II). Solutions with calcium chloride and HCl as Cl⁻ source were investigated with Cu:Cl ratios of 1:5 and 1:7, the 1:5 Cu:Cl ratio being the best performing. The substitution of calcium chloride with ammonium chloride increased the conductivity. However, while the effect on the positive electrode process was not very evident, the reversibility of the copper deposition-stripping process was greatly improved. Orthophosphoric acid could be a viable additive to decrease the complexation of calcium with chloride anions and to improve the stability of Cu(II) chloro-complexes. Absorption spectroscopy demonstrated that phosphate ions do not coordinate copper(II) but lead to a shift in the distribution of copper chloro-complexes toward more coordinated species. Electrochemically, the increased availability of chloride anions in solution stabilized the Cu(II)-rich solution and led to increased reversibility of the Cu(II)/Cu(I) redox process.



Citation: Lacarbonara, G.; Faggiano, L.; Porcu, S.; Ricci, P.C.; Rapino, S.; Casey, D.P.; Rohan, J.F.; Arbizzani, C. Copper Chloro-Complexes Concentrated Solutions: An Electrochemical Study. *Batteries* **2021**, *7*, 83. <https://doi.org/10.3390/batteries7040083>

Academic Editor: Elton J. Cairns

Received: 25 September 2021

Accepted: 1 December 2021

Published: 3 December 2021

Publisher’s Note: MDPI stays neutral with regard to jurisdictional claims in published maps and institutional affiliations.



Copyright: © 2021 by the authors. Licensee MDPI, Basel, Switzerland. This article is an open access article distributed under the terms and conditions of the Creative Commons Attribution (CC BY) license (<https://creativecommons.org/licenses/by/4.0/>).

1. Introduction

The interest in copper chloro-complexes is not new. CuCl solutions have enabled a more economical electrowinning process than CuSO₄ solutions, given that in CuCl electrolytes a one-electron process occurs at a lower potential [1]. In addition, concentrated brines have a role in geological field studies [2–4]. The application in alternative hydrometallurgical processes [5,6] has maintained a high interest in copper complexes. In the field of energy storage, several groups have actively pursued the development of thermochemical cycles for hydrogen production based on the Cu-Cl cycle in which the hydrogen is produced by the electrochemical reaction of the CuCl/HCl(aq) electrolyzer [7–10]. In addition, thermally regenerative ammonia batteries that convert low-grade waste heat into electrical power can use ligands to stabilize Cu(I) ions in the anolyte and catholyte chambers, achieving coulombic efficiencies above 90% [11].

In the field of batteries, the application of copper-complex chemistry was exploited for the first time in the mid-seventies [12,13]. In the last decade, there has been a renewed interest in copper-based batteries, specifically copper redox flow batteries (CuRFBs). The research, indeed, has been focused on different kinds of CuRFB, from thermally regeneration, based on the complexation of Cu⁺ with acetonitrile [14], to those operating with

deep eutectic solvents [15] or with highly concentrated chloride [16,17] or bromide [18] solutions. CuRFBs are more sustainable than redox flow batteries based on vanadium, for stationary application and for coupling with renewable energy sources. Within the variety of RFB that has been proposed since the seventies [19], vanadium based redox flow batteries (VRFB) have been the most studied and commercialized. However, the VRFB system employs toxic and high-cost materials, the latter including perfluorinated membranes as separators [20,21]. On the contrary, copper RFB can take advantage of the lower cost of copper with respect to that of vanadium, of the possibility of using other membranes than perfluorinated ones, and of the well-consolidated value chain in Europe of copper with respect to vanadium.

Copper halide-complexes play a crucial role in developing a highly performing CuRFB system. Specifically, their solubility and diffusion coefficients are of paramount importance in these systems. Copper bromo- and chloro-complexes have been investigated and the thermodynamic and kinetics parameters evaluated from dilute and concentrated copper solutions [22–29]. Stability constants were also evaluated in dilute solutions of copper chloride complexes [25]. It was found that in the presence of a high concentration of halides, Cu^+ and Cu^{2+} form halide-complexes with increasing halide content by increasing the number of halide ligands, up to CuX_3^{2-} and CuX_4^{2-} in complexes for Cu(I) and Cu(II), respectively [25,26]. The diffusion coefficients of Cu^+ and Cu^{2+} range from 10^{-5} to $10^{-6} \text{ cm}^2 \text{ s}^{-1}$, with higher values for higher temperatures and for Cu^+ than for Cu^{2+} , with a small variation for different X^- concentration [26].

However, the increase of the copper concentration, needed to achieve high energy RFB, brings a tremendous increase in the ionic strength of the solution needed to maintain a suitable copper-to-halide ratio. In these conditions, the interactions between ions are more intense, and the decrease of water activity strongly affects physicochemical parameters like viscosity and density, as well as conductivity and the diffusion coefficient. Several studies have been carried out in concentrated solutions of copper halides in electrolyzer technology for hydrogen production to evaluate the thermodynamic parameters [8,9,27–29]. The diffusion coefficients of Cu(II) chlorocomplexes at 40°C in 2 M CuCl_2 solutions were found to be in the range 10^{-5} to $10^{-7} \text{ cm}^2 \text{ s}^{-1}$ depending on the solution composition [16,30–32]. The lowest values were achieved with an increase of Cl^- concentration by changing the Cl^- source from HCl to CaCl_2 while maintaining the Cu:Cl ratio constant [30].

In order to achieve RFB technology with high performance and cycle life, the total concentration of copper and chloride in the electrolytes must be considered. Sanz et al. [16] demonstrated that a Cu:Cl ratio of 1:5 is mandatory to ensure salt solubility and cuprous cation stability by Cl-complexation. The choice of the chloride sources as supporting electrolytes influences the physical properties of the copper-chloride electrolytes and the electrochemical properties of the Cu(II)/Cu(I) redox couple. The use of HCl or CaCl_2 alone as supporting electrolyte limits the minimum temperature and the electrolyte concentration at which the solution does not show precipitates. On the contrary, solutions containing both HCl and CaCl_2 are stable without precipitates over a wide range of temperatures, from 5 to 70°C , affording their practical application in the CuRFB [16,17,30].

The aim of this study was to investigate copper concentrated solutions of interest for CuRFB in order to optimize cell performance. We report and discuss the results of the physicochemical and electrochemical characterization of 2 M solutions of Cu(I) and Cu(II) with copper to chloride ratios of 1:5 and 1:7, where the concentration and the counter-ion of the chloride complexing agent are varied. The cell operating temperature was maintained between 40°C and 60°C to reproduce the real operating conditions of RFB, where low temperatures are preferable to reduce system heating costs. The low temperature range requires that the state of charge (SoC) never exceeds 90% to avoid CuCl_2 precipitation. In addition, in concentrated CuCl solutions the pH must be controlled to allow for total solubilization of the salt. For this reason, the HCl concentration was maintained at 6 M.

2. Results and Discussion

2.1. Solutions with Calcium Chloride

Solutions with only CuCl or CuCl₂ as copper salt, and solutions with copper concentration shared between CuCl and CuCl₂ to simulate the 0%, 100%, and 50% SoC, with Cu:Cl ratios 1:5 and 1:7, were selected and analyzed with a view to CuRFB technology. While physicochemical parameters have an impact on the energy consumption of the CuRFB hydraulic system, electrochemical properties are fundamental in determining the reaction kinetics and overall battery performance.

Table 1 summarize the composition of the solutions 1–6 (from here on indicated with a number) containing CaCl₂, the conductivity, the viscosity, and the density at 40 °C, while Figure 1 shows the above parameters at different temperatures.

Table 1. Physicochemical properties at 40 °C of copper electrolytes with different concentrations of copper and calcium chloride with Cu:Cl ratios of 1:5 and 1:7. The relative errors of conductivity, viscosity, and density measurements are 0.5%, 0.35%, and 0.1%, respectively.

<i>n</i>	CuCl ₂ M	CuCl M	CaCl ₂ M	HCl M	Cu:Cl	σ mS cm ⁻¹	η mPa s	ρ kg m ⁻³
1	/	2	1	6	1:5	634	1.41	1312
2	1	1	0.5	6	1:5	605	1.78	1291
3	2	/	/	6	1:5	645	1.38	1308
4	/	2	3	6	1:7	364	2.80	1442
5	1	1	2.5	6	1:7	359	2.93	1431
6	2	/	2	6	1:7	417	2.10	1404

Solutions with low Cl[−] concentration (1–3, Cu:Cl ratio 1:5) show higher conductivity (Figure 1a) than the solutions with high Cl[−] concentration (4–6, Cu:Cl ratio 1:7). The addition of an increasing amount of CaCl₂ causes a significant increase in viscosity and density (Figure 1b,c). Solution 6 was the best performing with Cu:Cl 1:7 ratio, accordingly with a lower concentration of CaCl₂ than solutions 4 and 5.

Figure 2 shows the CVs of the 1–6 solutions carried out at 40 °C and 0.1 V s^{−1}. Our systems are quasi reversible. They do not display a Nernstian reversibility, given that the separation between the cathodic and the anodic peak potentials (ΔE) is higher than 2.22 RT/F (59 mV at 40 °C) [33]. However, we focused our attention on the i_{pa}/i_{pc} ratio that for a totally reversible system must be 1, independent of the scan rate [34]. This denotes whether an active species can be subsequently reduced and oxidized.

Solutions 1–3 (Figure 2a) shows lower separation between the anodic and cathodic peaks (ΔE) with respect to the 4–6 solutions (Figure 2b). In particular, the reversibility is higher for solution 3, without CaCl₂, and for the mixed Cu⁺/Cu²⁺ solution 2. Solution 5 also displays an i_{pa}/i_{pc} ratio near 1 even if the ΔE is higher, probably due to the low conductivity and high viscosity.

Data from CVs are collected in Table 2 that reports the open circuit potential vs. SCE (OCP), the peak potentials vs. saturated calomel electrode (SCE) of the anodic and cathodic processes (E_+ and E_-), the separation between the peak potentials (ΔE), the potential of the redox couple Cu⁺/Cu²⁺ calculated by the half-sum of the peak potentials, and the anodic and cathodic peak current densities (i_{pa} and i_{pc}) and their ratios.

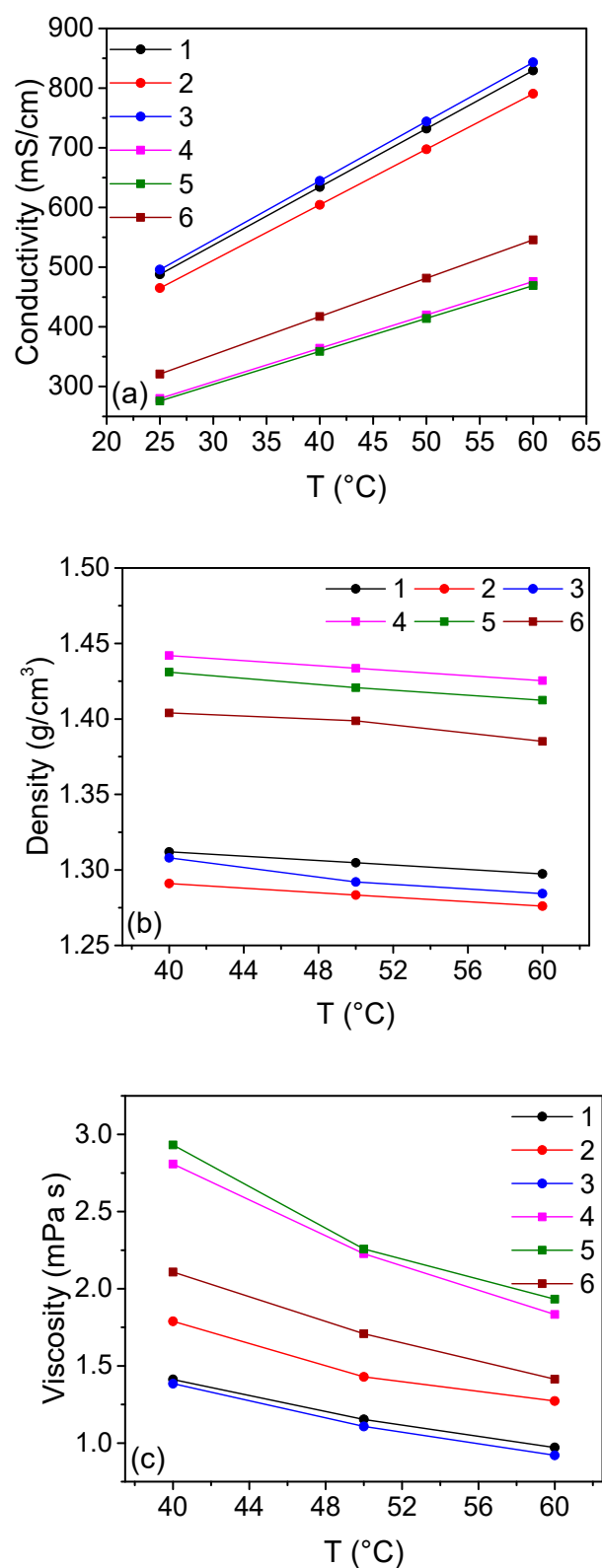


Figure 1. Conductivity (a), density (b), and viscosity (c) of copper electrolytes with Cu:Cl ratios of 1:5 (solutions 1–3) and 1:7 (solutions 4–6) at different temperatures. The solution total copper and HCl concentrations were 2 M and 6 M, respectively. Solution compositions are shown in Table 1.

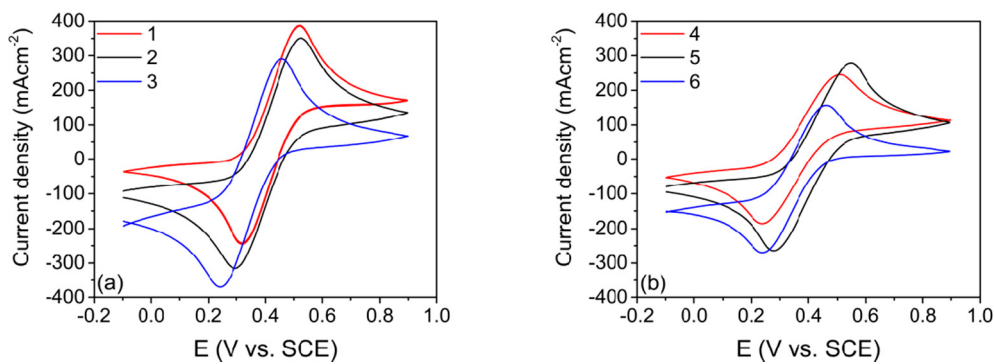


Figure 2. CVs of the GC electrode in solutions with different concentrations of copper and calcium chloride with Cu:Cl ratio 1:5 (a) and 1:7 (b) at 0.1 V s^{-1} and 40°C .

Table 2. Electrochemical properties on GC at 0.01 V s^{-1} and 40°C of copper electrolytes with different concentrations of copper and calcium chloride for Cu:Cl ratios of 1:5 (solutions 1–3) and 1:7 (solutions 4–6). The relative errors of potential measurements are ca. 0.5% and those related to the current measurements are ca. 1%.

<i>n</i>	OCP V vs. SCE	E_+ V vs. SCE	E_- V vs. SCE	ΔE V	$(E_+ + E_-)/2$ V	i_{pa} mA cm^{-2}	i_{pc} mA cm^{-2}	i_{pa}/i_{pc}
1	0.309	0.483	0.347	0.136	0.415	149	-171	0.87
2	0.409	0.469	0.340	0.129	0.405	162	-163	0.99
3	0.622	0.419	0.299	0.120	0.359	151	-151	1
4	0.302	0.447	0.296	0.151	0.372	112	-107	1.05
5	0.417	0.481	0.340	0.141	0.411	117	-118	0.99
6	0.525	0.430	0.293	0.137	0.362	107	-113	0.95

The combination of HCl with CaCl_2 with Cu:Cl ratio 1:5 seems the most promising in terms of conductivity, viscosity, and density as positive copper-chloride electrolytes.

However, Cl^- concentration plays a crucial role in the copper speciation considering that the formation constant for CuCl_x^{2-x} depends on it. By adding calcium chloride, the chloride concentration, i.e., the availability of complexing agents for copper, should be increased. The $(E_+ + E_-)/2$ does not change significantly when the chloride concentration increases. In high concentrated solution, calcium chloride is not completely dissociated [35] and theoretical work [36] has shown that Ca^{2+} can coordinate chloride to form chloro-complexes even if the $[\text{CaCl}_x]^{2-x}$ ($x = 4\text{--}6$) clusters become metastable when hydration is considered. The high ionic strength of the solution used implies a low water content for the complete solvation of calcium.

Hence, to increase the chloride availability in copper solutions and improve the solutions' chemical-physical properties, two main approaches are outlined. The former is the use of a different chloride source, CaCl_2 concentration representing the critical factor in terms of conductivity and viscosity as shown for solutions 4–6. The latter is the use of an additive able to interact with Ca^{2+} and, in turn, to weaken the interaction between Ca^{2+} and Cl^- .

2.2. Solutions Containing NH_4Cl as Chloride Source

The chloride salts and additive selection for CuRFB technology is not very wide because of solubility and overall sustainability. CaCl_2 was the preferred source of chloride ions in previous works due to its high solubility, low cost, and availability, being also a bi-equivalent source of chloride. However, a high amount of calcium chloride leads to increased viscosity and density, which adversely impacts the electrolyte hydraulic circuit of the CuRFB, as well as to a decreased conductivity.

Among the different chloride salts, NH_4Cl shows high solubility in water and low cost. The solutions 7 and 8 were prepared by replacing calcium chloride with ammonium

chloride, as shown in Table 3, and Figure 3 displays conductivity, density, and viscosity at different temperatures. The conductivity (Figure 3a) of solutions 7 and 8 are significantly higher than that of the corresponding solution with CaCl_2 (solutions 1 and 2). The density (Figure 3b) and the viscosity (Figure 3c) values are comparable and even lower than those of solutions 1 and 2 (Table 1).

Table 3. Physicochemical properties at 40 °C and 60 °C of copper electrolytes with different concentrations of copper and ammonium chloride with Cu:Cl ratio of 1:5. The relative errors of conductivity, viscosity, and density measurements are 0.5%, 0.35%, and 0.1%, respectively.

<i>n</i>	T °C	CuCl_2 M	CuCl M	CaCl_2 M	HCl M	NH_4Cl M	Cu:Cl	σ mS cm^{-1}	η mPa s	ρ kg m^{-3}
7a	40	/	2	/	6	2	1:5	812	1.08	1296
7b	60	/	2	/	6	2	1:5	1003	0.76	1283
8a	40	1	1	/	6	1	1:5	819	1.33	1250
8b	60	1	1	/	6	1	1:5	1012	0.83	1236

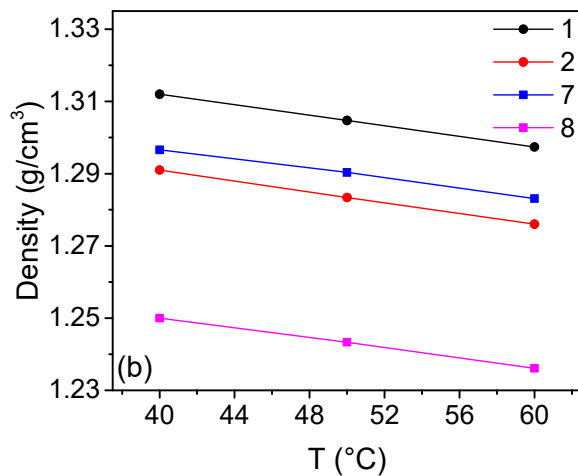
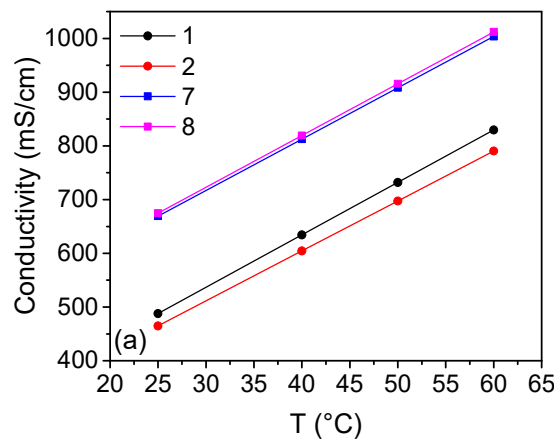


Figure 3. Cont.

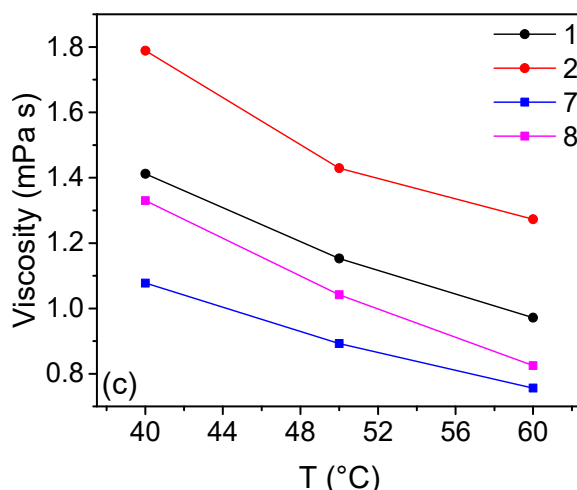


Figure 3. Conductivity (a), density (b), and viscosity (c) of copper electrolytes with Cu:Cl ratio of 1:5 (solutions 7 and 8, see Table 3) at different temperatures. The total copper and HCl concentrations were 2 M and 6 M, respectively.

The CVs reported in Figure 4a,b for the solutions 7a and 8a at 40 °C show a resistive shape due to crystal precipitation on the electrode surface during the reduction. CVs became more reversible by increasing the temperature up to 60 °C (solution 7b) with an i_{pa}/i_{pc} ratio near 1. Also ΔE values decreased both in the Cu(I) and in the Cu(I)/Cu(II) solutions at 60 °C. Additionally, by increasing the temperature, the potentials shifted toward positive values, as shown in Table 4 which shows the electrochemical parameters of solutions 7 and 8 at 40 °C and 60 °C.

From the electrochemical results, it is evident that, despite the good physicochemical properties, the solutions with NH₄Cl are not preferable to those with CaCl₂ in the positive half-cell of the CuRFB. On the other hand, looking at the deposition–stripping processes occurring in solution 7b compared to those in solution 1, the addition of ammonium chloride to the electrolyte greatly improved the coulombic efficiency (CE) evaluated by the ratio between the stripping and deposition charges. CVs in the potential range of copper deposition–stripping in the electrolyte with calcium chloride (solution 1, Figure 4c) revealed a CE around 50% on the GC electrode. After 10 consecutive cycles, the potential at which the copper deposition starts drops from 0.325 V to 0.300 V vs. SCE due to the incomplete stripping of copper deposit.

On adding NH₄Cl to the electrolyte (solution 7b, Figure 4d), the CE increased to 85% and the overpotential of the copper deposition results were unvaried upon cycling. The addition of NH₄Cl to the negative half-cell electrolyte led to increased reversibility of the negative process by restoring the electrode surface after the copper stripping. It is worth noting that ammonium chloride is used in metalworks for polishing metal surfaces by metal oxides [37] and it could be very useful for improving the performance of the negative half-cell in CuRFB.

Figure 4e,f show the SEM images of copper deposited on Sigracell FR10 graphite at 80 mA cm⁻² for 1200 s at 60 °C in solution 1 and solution 7b. The images show that smaller grain copper deposits are achieved from the calcium chloride (solution 1) while a larger grain deposit is observed with the ammonium chloride (solution 7b) based electrolyte. The deposits from solution 1 also appear to have more isolated (some triangular type) crystalline features which could be detached from the surface during dissolution without contributing to the efficiency of the reaction. The more coherent deposit from solution 7b may explain why a significantly higher CE is attained in that electrolyte.

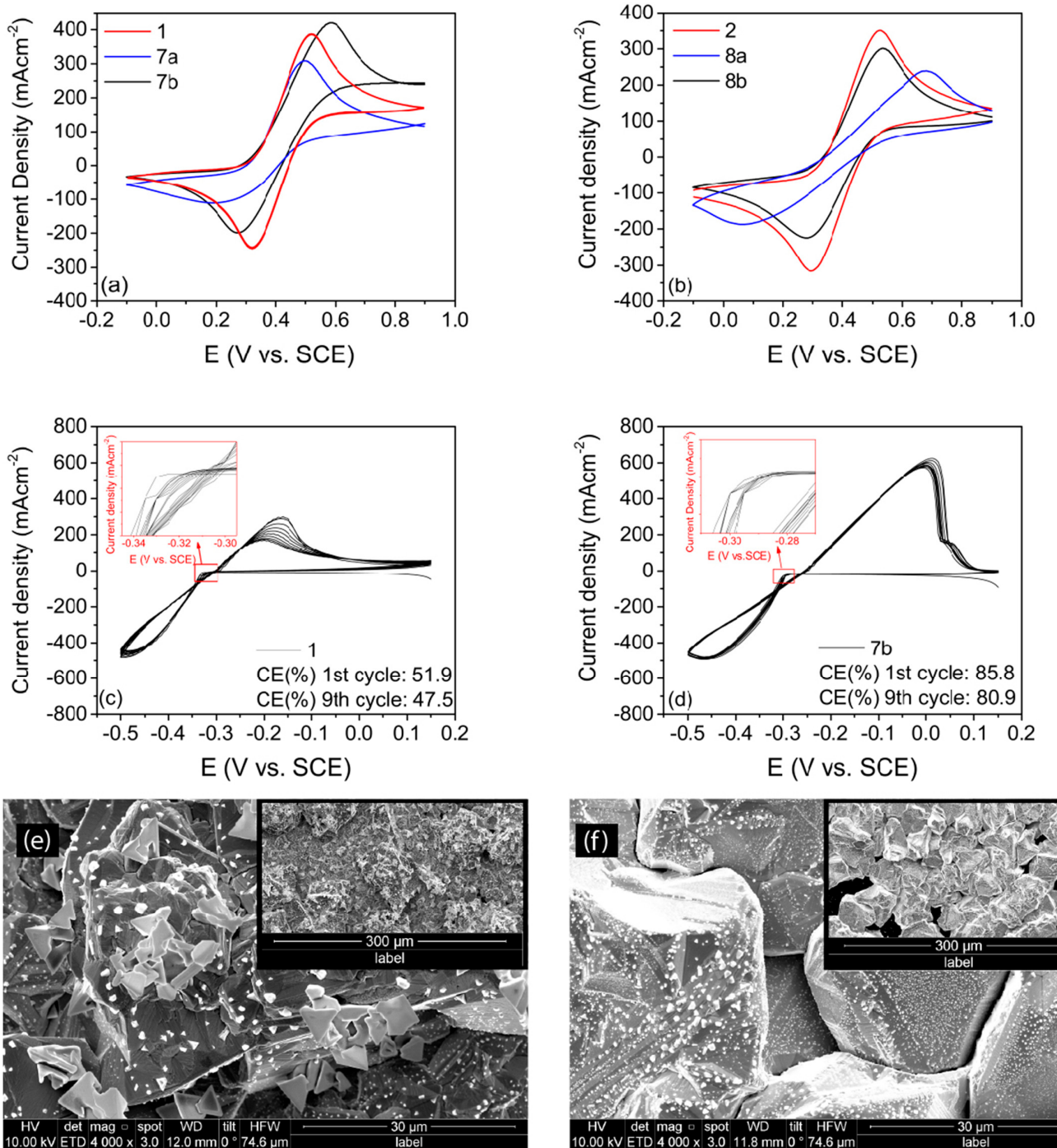


Figure 4. CVs of GC electrode at 0.1 V s⁻¹ of (a) the solution 1, 7 and (b) 2, 8 in which 1,2, 7a, and 8a were carried out at 40 °C, while 7b and 8b were at 60 °C; Cu deposition stripping at 0.1 V s⁻¹ and 60 °C of (c) solution 1 and (d) solution 7b; SEM images (4000×) of copper deposited at 60 °C in solution 1 (e) and in solution 7b (f). In the inset are the images at 400× magnification.

Table 4. Electrochemical properties on GC at 0.01 V s^{-1} and 40°C and 60°C of copper electrolytes with different concentrations of copper and NH_4Cl with a Cu:Cl ratio of 1:5. The relative errors of potential measurements are ca. 0.5% and those related to the current measurements are ca. 1%.

n	T $^\circ\text{C}$	OCP V vs. SCE	E_+ V vs. SCE	E_- V vs. SCE	ΔE V	$(E_+ + E_-)/2$ V	i_{pa} mA/cm^{-2}	i_{pc} mA cm^{-2}	i_{pa}/i_{pc}
7a	40	0.324	0.548	0.283	0.265	0.416	150	-126	1.19
7b	60	0.324	0.550	0.309	0.241	0.430	211	-216	0.98
8a	40	0.375	0.528	0.270	0.258	0.399	125	-143	0.87
8b	60	0.380	0.484	0.326	0.158	0.405	146	-170	0.86

Diffusion coefficients were evaluated for selected solutions by chronoamperometric techniques at a potential of ($i_{pa} + 0.1 \text{ V}$) vs. SCE for Cu(I) oxidation or ($i_{pc} - 0.1 \text{ V}$) vs. SCE for Cu(II) reduction. The tests were carried out with a GC working electrode (3 mm diameter) to avoid the contribution of edge effects originating from radial contributions [38].

Figure 5 shows the chronoamperometric curves of the solutions 1, 4, and 7a at 40°C and the fitting of the curves i vs. $t^{-1/2}$ according to the Cottrell equation in a time range from 0.5 s to 2 s. As shown in Figure 5b, solution 4 has the lowest diffusion coefficient, even lower than solution 1. The presence of two cations with interconnected equilibria of complexation with the same ligand can decrease the coordination. Less coordinated complexes can show higher diffusion coefficients due to a smaller radius. However, increasing the concentration of calcium chloride, i.e., on increasing the Cu:Cl ratio from 1:5 to 1:7, the diffusion coefficients decrease. The increase of the ionic strength of the solutions decreases the mobility of the ions. As previously discussed, increasing the Cu:Cl ratio from 1:5 to 1:7 is not beneficial for electrochemical performance. On substituting the CaCl_2 with NH_4Cl , the diffusion coefficient increases as a consequence of the lower viscosity of solution 7a with respect to solution 1, given that NH_4^+ is a water destructuring ion. This confirms the suitability of ammonium chloride as a chloride source for the negative half-cell.

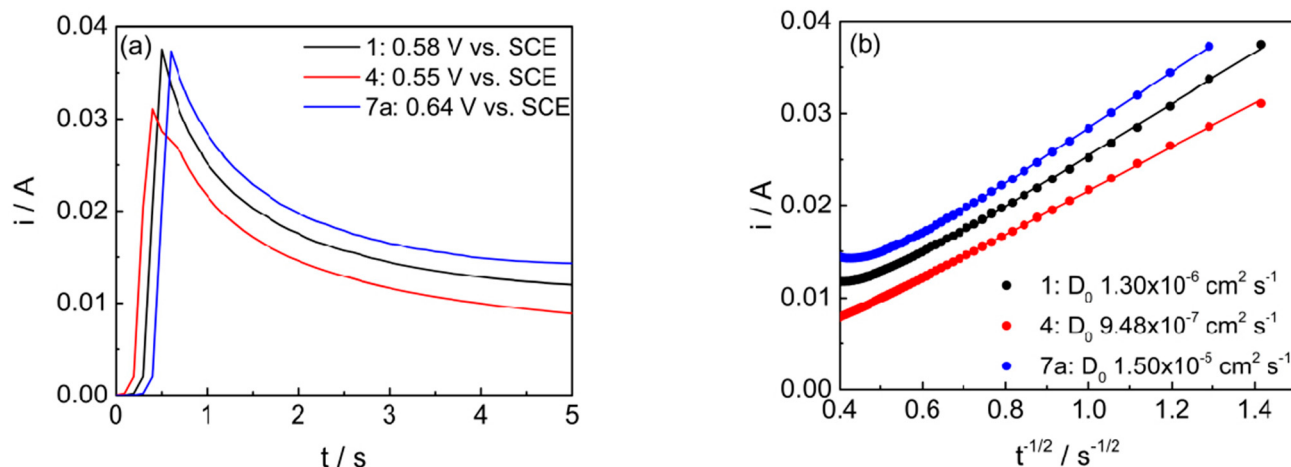


Figure 5. (a) Chronoamperometric curves at ($i_{pa} + 0.1 \text{ V}$ vs. SCE) of solutions 1, 4 and 7. (b) fitting of the curves i vs. $t^{-1/2}$ according to the Cottrell equation in a time range from 0.5 s to 2 s (b).

2.3. Solutions Containing H_3PO_4 as Additive

Additives including big anions can influence the equilibria of Cu^+ and Ca^{2+} chloro-complexes. As an example, Ca^{2+} and PO_4^{3-} interact and CaCl_2 and H_3PO_4 are used as precursors for the formation of calcium phosphates [39]. For this reason, orthophosphoric acid can be used to decrease the calcium chloride coordination. Ca^{2+} chloro-complexes become destabilized, and the “free” Cl^- can shift the equilibrium of the copper complex formation toward a more coordinated species. Additionally, the introduction of protons

instead of other cations could be favorable for the conductivity and to avoid further foreign species in the electrolyte.

Two solutions containing H_3PO_4 were prepared: solution 10, where H_3PO_4 was added to formulation 1 (0% SoC), and solution 11, in which both $CuCl$ and $CuCl_2$ were present, and where $CaCl_2$ had a concentration of 1 M for a better comparison with solutions 1 and 10. Considering that, in the RFB system, the SoC is limited at 90%, the mixed Cu^+/Cu^{2+} solutions prepared should mimic the 90% SoC. To investigate the effect of phosphate on calcium chloride dissociation, solution 9 with the same composition as solution 11 without H_3PO_4 was also prepared. Table 5 reports the physicochemical parameters of these solutions with and without H_3PO_4 additive.

Table 5. Physico-chemical properties on GC at 0.01 V s^{-1} and $40\text{ }^\circ\text{C}$ of copper electrolytes with different concentrations of copper and H_3PO_4 with $Cu:Cl$ ratio of 1:5. The relative errors of conductivity, viscosity, and density measurements are 0.5%, 0.35%, and 0.1%, respectively.

<i>n</i>	$CuCl_2$ M	$CuCl$ M	$CaCl_2$ M	HCl M	H_3PO_4 M	$Cu:Cl$	σ $mS\text{ cm}^{-1}$	η $mPa\text{ s}$	ρ $kg\text{ m}^{-3}$
1	/	2	1	6	/	1:5	634	1.41	1312
9	1.8	0.2	1	6	/	1:5.9	569	1.73	1347
10	/	2	1	6	1	1:5	714	1.62	1300
11	1.8	0.2	1	6	1	1:5.9	508	1.66	1334

Figure 6 summarizes the results of conductivity, density, and viscosity at different temperatures of the solution reported in Table 5.

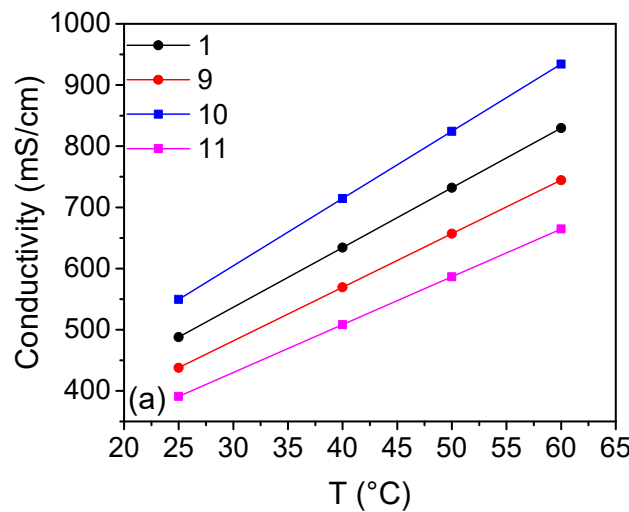


Figure 6. Cont.

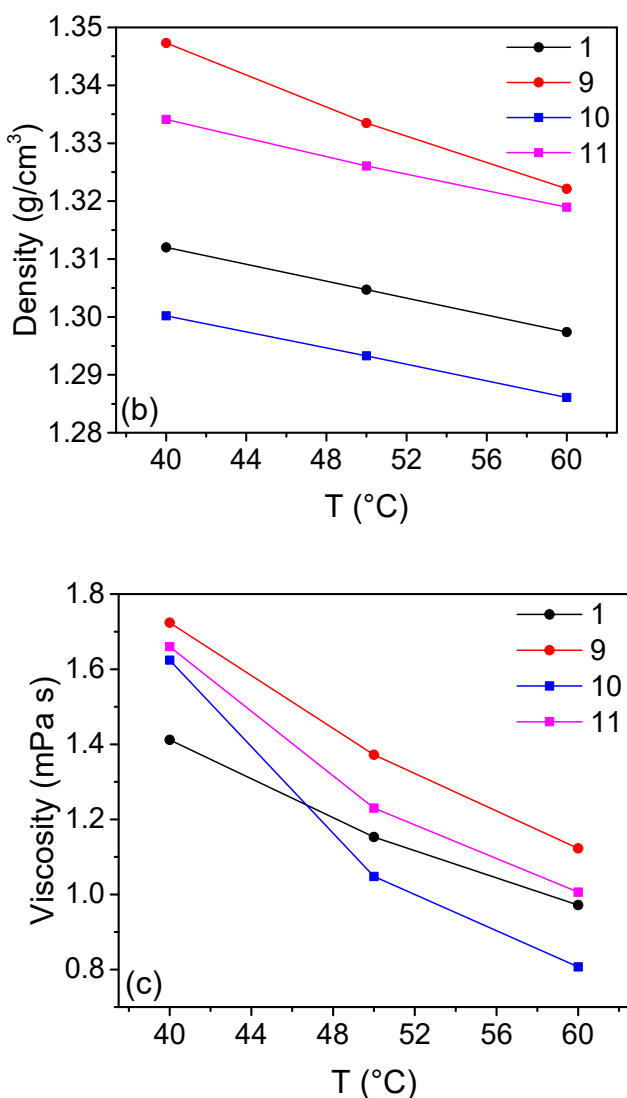


Figure 6. Conductivity (a), density (b), and viscosity (c) of copper electrolytes with Cu:Cl ratio of 1:5 (solutions 1 and 9 without H_3PO_4 , and solution 10 and 11, with H_3PO_4) at different temperatures. The total copper and HCl concentrations were 2 M and 6 M, respectively.

Figure 6 shows that the addition of phosphoric acid to formulation 1 (solution 10) leads to a conductivity increase, due to the increase in H_3O^+ concentration, despite a higher viscosity. The parameters of the solutions show the opposite trend for solutions 9 and 11, with a decreased conductivity for solution 11 and a slight decrease of density and viscosity with respect to solution 9. The latter solutions have higher ionic strength (Cu:Cl ratio of 1:5.9) than the solutions 1 and 10, and the addition of phosphoric acid further increases it. In this case, presumably, the conduction mechanism of H_3O^+ is hindered by the increase of Cl^- concentration, Cl^- being a water-destructuring ion.

Table 6 reports the electrochemical properties of the solutions of Table 5 while Figure 7 displays the CVs at 40 °C. For the solution of Cu(I) (Figure 7a), the addition of orthophosphoric acid increases and improves the reversibility of the CV (i_{pa}/i_{pc} ratio), with the potential of the redox couple shifted towards less positive values. In highly concentrated Cu(II) electrolytes, the reversibility results increased (Figure 7b) despite the lower conductivity of solution 11 with respect to 9. The ΔE is reduced from 268 mV to 167 mV and, the i_{pa}/i_{pc} ratio approaches 1.

Table 6. Electrochemical properties at 40 °C of copper electrolytes with CaCl_2 , with and without H_3PO_4 with a Cu:Cl ratio of 1:5. The relative errors of potential measurements are ca. 0.5% and those related to the current measurements are ca. 1%.

<i>n</i>	OCP V vs. SCE	E_+ V vs. SCE	E_- V vs. SCE	ΔE V	$(E_+ + E_-)/2$ V	i_{pa} mA cm^{-2}	i_{pc} mA cm^{-2}	i_{pa}/i_{pc}
1	0.309	0.483	0.347	0.136	0.415	149	-171	0.87
9	0.490	0.477	0.209	0.268	0.343	127	-120	1.06
10	0.297	0.473	0.309	0.164	0.391	142	-154	0.92
11	0.427	0.444	0.277	0.167	0.361	125	-120	1.04

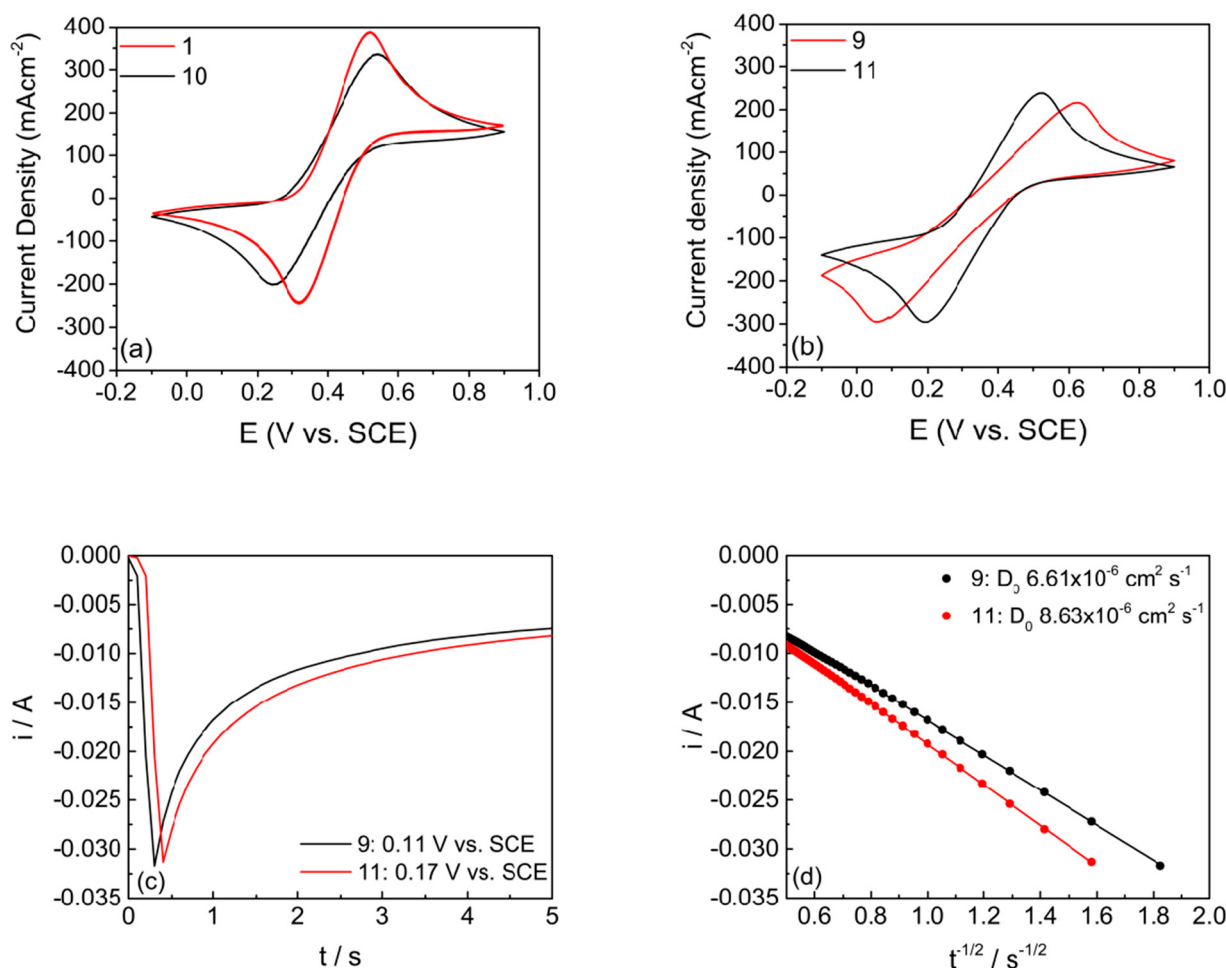


Figure 7. CVs of GC electrode at 0.1 V s^{-1} and 40 °C in solutions with different concentrations of copper and calcium chloride with and without H_3PO_4 (a) at 0% SoC and (b) at 90% SoC. (c) Chronoamperometric curves of Cu(II) at ($i_{pc} = 0.1 \text{ V}$ vs. SCE of 9 and 11 solutions (0% SoC), (d) fitting of the curves i vs. $t^{-1/2}$ according to the Cottrell equation in a time range from 0.5 s to 2 s.

In solutions with a chloride concentration higher than 5M, Cu(I) is preferentially present as the most chloro-coordinated species CuCl_3^{2-} [3]. The increased availability of chloride ligands is more effective for Cu(II)-rich electrolytes. Under the same conditions, Cu(II) chlorocomplexes favour the lower coordination number, and changes in chloride concentration, even at high ligand concentration, can affect the copper chlorocomplex distribution [25]. Hence, copper(I) is less affected by a higher amount of uncomplexed chloride anions than Cu(II). In oxidized solutions, the chloride released due to the presence

of phosphoric acid can coordinate the Cu(II) cations leading to a more reversible and electrochemically stable redox couple.

In solution 9 with 1.8 M Cu(II), the diffusion coefficient obtained from the Cottrell equation (Figure 7c,d) increases with the addition of 1 M H₃PO₄ even as the conductivity of the solution decreases from 569 mS cm⁻¹ to 508 mS cm⁻¹ as a consequence of the higher ionic strength. As observed in the CV measurements, H₃PO₄ is more effective in the Cu(II) chemical environment with respect to the copper(I). Hence, the Cu(II) diffusion coefficient varies from 6.6×10^{-6} cm² s⁻¹ to 8.6×10^{-6} cm² s⁻¹.

Absorption spectroscopy of Cu(II) halide-complexes has been intensively studied in both aqueous and organic solvents [4,40–42]. The absorption spectrum of copper (II) is characterized by two transitions. In the UV region, the ligand-to-metal charge transfer (LMCT) transition contains information about the degree of complexation, while in the NIR there is a broad metal centered (MC) band (d-d transition) which is harder to resolve.

The LMCT is too intense in highly concentrated solution, hence, changes in the coordination sphere are established from the MC band. From the crystal field theory, ligands modify the ligand-field splitting parameter Δ that determines the energy of the MC transition. The presence of chloride ligands in the copper coordination sphere reduces the Δ and red shift of the MC band with respect to aquo-complex [43].

Figure 8a reports the absorption spectrum in the Vis/NIR region of the high concentrated Cu(II)/Cu(I) solution with the unvaried concentration of CaCl₂, i.e., solutions 9 and 11.

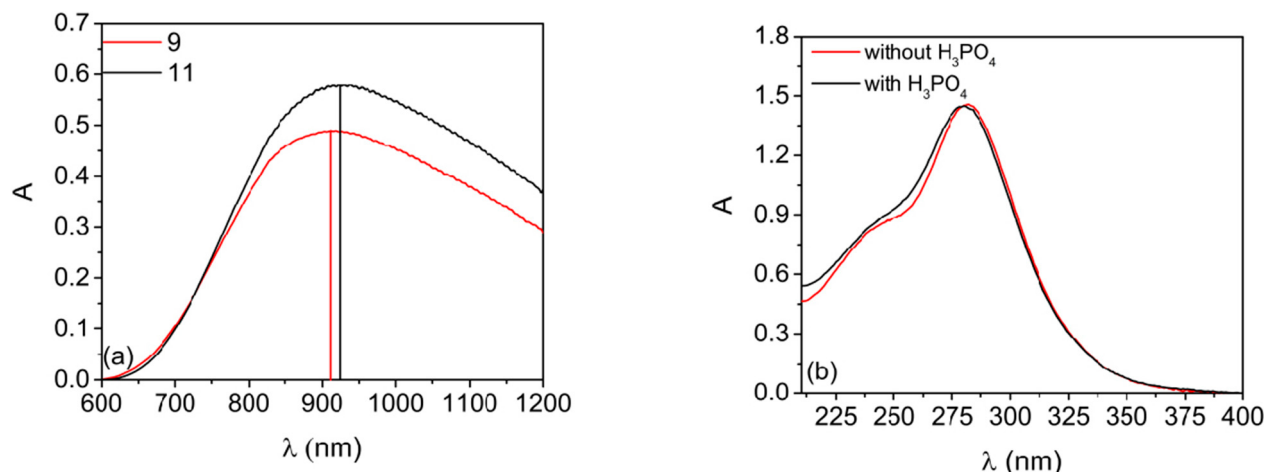


Figure 8. Absorption spectra: (a) MC band of concentrated 9 and 11 solutions with optical path of 50 μ m and (b) LMCT band of 10 mM CuCl₂, 10 mM CaCl₂, 30 mM HCl with and without 10 mM H₃PO₄ (optical path 500 μ m).

The addition of H₃PO₄ leads to a red shift of MC from 925 nm to 910 nm. According to deconvolution of the MC band [4], this shift can be interpreted as a decrease of low chloride-coordinated complexes and an increase of the component for CuCl₃⁻. Differences in absorbance are justified by the different molar extinction coefficients of the complexes involved. On the other hand, phosphate anions do not enter the inner coordination sphere of the copper [44] as demonstrated by the spectra in Figure 8b of a diluted solution (200 times) with the same composition of solutions 9 and 11. These spectra show the LMCT bands with an unvaried presence of CuCl₃⁻.

3. Materials and Methods

For the solutions CuCl₂ (>99.99%, Sigma Aldrich), CuCl (\geq 99.995% trace metal basis, Sigma Aldrich, HCl (37%, Sigma-Aldrich, Merck KGaA, Darmstadt, Germany), CaCl₂ (\geq 99%, ACS reagent, Sigma Aldrich, Merck KGaA, Darmstadt, Germany), NH₄Cl (99.5%, Sigma Aldrich, Merck KGaA, Darmstadt, Germany) and H₃PO₄ (\geq 85 wt% solution in water, ACS reagent, Sigma Aldrich, Merck KGaA, Darmstadt, Germany) were used. After

complete dissolution in deionized water, the solutions were deaerated with Ar for ten minutes and sealed. The solution composition is given in the tables in the results and discussion section, and the solutions are indicated with a number. Conductivity tests were carried out with Sension + EC71 Hach Instruments (Hach Lange GmbH, Düsseldorf, Germany), viscosity tests were performed with SVM 3000 Stabinger Anton Paar (Anton Paar GmbH, Graz, Austria), and density was measured by DMA 4500 Anton Paar (Anton Paar GmbH, Graz, Austria) at different temperatures. Electrochemical tests were carried out under Ar atmosphere in a conventional V-cell, kept in a water bath at 40 °C, with a Voltalab PGZ301 (Radiometer, Copenhagen, Denmark). The cell contained 10 mL solution. A glassy carbon (GC, 3 mm diameter) was used as the working electrode, a graphite rod (6 mm diameter, 15 cm length, Gamry Instruments, Warminster, PA, USA) as counter electrode and a saturated calomel electrode (SCE, 303/SCG/6J, AMEL, Milan, Italy) as reference electrode. Cyclic voltammetry (CVs) studies were carried out at 40 °C at different scan rates, from 0.1 to 0.005 V s⁻¹. CVs in solutions containing NH₄Cl were performed at 60 °C. The voltammograms are not live-IR corrected. Scanning Electron Microscopy (SEM) images were collected with an FEI Quanta 650 Scanning Electron Microscope (FEI, Hillsboro, OR, USA). Spectrophotometric tests were performed with a Perkin Elmer Lambda 19 (Perkin Elmer Italia SpA, Milan, Italy) in quartz cells with an optical path length of 50 μm in the ultraviolet-visible (UV-Vis) region and 500 μm in the near infrared (NIR) region.

4. Conclusions

In relation to the growing interest in RFB systems and copper chemistry in solution, different copper electrolytes were characterized for application in CuRFB. The effect of calcium chloride as supporting electrolyte was tested in solution with a Cu:Cl ratio of 1:5 and 1:7. Solutions with 1:5 Cu:Cl ratio displayed the best performance. The substitution of calcium chloride with ammonium chloride increased the conductivity up to 1000 mS cm⁻¹ without improving the Cu(I)/Cu(II) couple redox processes. On the other hand, the addition of NH₄Cl to Cu(I) electrolyte led to improved reversibility of the copper deposition–stripping processes with CE reaching 80%.

The interaction of phosphate with Ca²⁺ suggested that H₃PO₄ could be a viable additive to decrease the complexation of calcium with chloride and to improve Cu(II) chlоро-complex stability. UV-VIS spectroscopy demonstrated that phosphate does not take part in the coordination sphere of Cu(II). The addition of H₃PO₄ in concentrated solution led to a shift in the distribution of copper cholorocomplexes toward more coordinated species visible in the NIR absorption spectrum. Electrochemically, the addition of phosphoric acid is not effective on Cu(I)-rich electrolyte due to the lower amount of chloride required for coordination. The increased availability of chloride anions in solution stabilizes the Cu(II)-rich solution and leads to increased reversibility of the Cu(II)/Cu(I) redox process and higher copper(II) diffusion coefficients.

Author Contributions: Conceptualization, C.A. and G.L.; methodology, G.L., L.F.; experimental investigation and validation, G.L., L.F., S.P., D.P.C.; formal analysis, S.R., J.F.R., P.C.R.; writing—original draft preparation, G.L.; writing—review and editing, C.A., S.R., P.C.R., J.F.R.; supervision, C.A.; project administration, C.A., P.C.R., J.F.R.; funding acquisition, C.A., P.C.R., J.F.R. All authors have read and agreed to the published version of the manuscript.

Funding: This work was supported by the European Union within the Horizon 2020 research and innovation programme [CUBER—Copper-Based Flow Battery for Energy storage Renewables Integration H2020-LC-BAT_2019] under grant agreement No. 875605. G.L. acknowledges the Department of Excellence program financed by the Minister of Education, University and Research (MIUR, L. 232 del 01/12/2016) for the doctoral scholarship.

Institutional Review Board Statement: Not applicable.

Informed Consent Statement: Not applicable.

Data Availability Statement: All the date are included in the paper.

Acknowledgments: All the Project Partners are acknowledged for the fruitful discussion. The Authors thank Lorraine C. Nagle for SEM images.

Conflicts of Interest: The authors declare no conflict of interest.

References

- Mussler, R.E.; Campbell, T.T.; Olsen, R.S. Electrowinning of Copper from Chloride Solutions *U.S. Dept. of Interior, Bureau of Mines, Report of Investigation 8076*, Washington: 1975. Available online: <http://books.google.com> (accessed on 30 November 2021).
- Sugasaka, K.; Fujii, A. A Spectrophotometric Study of Copper(I) Chloro-Complexes in Aqueous 5M Na(Cl,ClO₄) Solutions. *Bull. Chem. Soc. Jpn.* **1976**, *42*, 82–86. [CrossRef]
- Fritz, J.J. Chloride Complexes of CuCl in Aqueous Solution. *J. Phys. Chem.* **1980**, *84*, 2241–2246. [CrossRef]
- Brugger, J.; McPhail, D.C.; Black, J.; Spiccia, L. Complexation of metal ions in brines: Application of electronic spectroscopy in the study of the Cu(II)-LiCl-H₂O system between 25 and 90 °C. *Geoch. Cosmoch. Acta* **2001**, *65*, 2691–2708. [CrossRef]
- Hyvärinen, O.; Hämäläinen, M.; Lamberg, P.; Liipo, J. Recovering Gold from Copper Concentrate via the HydroCopper™ Process. *JOM* **2004**, *56*, 57–59. [CrossRef]
- Lundström, M.; Aromaa, J.; Forsén, O.; Hyvärinen, O.; Barker, M.H. Cathodic reactions of Cu²⁺ in cupric chloride solution. *Hydrometallurgy* **2007**, *85*, 9–16. [CrossRef]
- Naterer, G.; Suppiah, S.; Lewis, M.; Gabriel, K.; Dincer, I.; Rosen, M. Recent Canadian advances in nuclear-based hydrogen production and the thermochemical Cu–Cl cycle. *Int. J. Hydrogen Energy* **2009**, *34*, 2901–2917. [CrossRef]
- Trevani, L.; Ehlerova, J.; Sedlbauer, J.; Tremaine, P.R. Complexation in the Cu(II)-LiCl-H₂O system at temperatures to 423 K by UV-Visible spectroscopy. *Int. J. Hydrogen Energy* **2010**, *35*, 4893–4900. [CrossRef]
- Soltani, R.; Dincer, I.; Rosen, M.A. Electrochemical analysis of a HCl(aq)/CuCl(aq) electrolyzer: Equilibrium thermodynamics. *Int. J. Hydrogen Energy* **2016**, *41*, 19, 7835–7847. [CrossRef]
- Farsi, A.; Zamfirescu, C.; Dincer, I.; Naterer, G.F. Electrochemical Transport in CuCl/HCl(aq) Electrolyzer Cells and Stack of the Cu–Cl Cycle. *J. Electrochem. Soc.* **2020**, *167*, 044515. [CrossRef]
- Springer, R.; Cross, N.R.; Lvov, S.N.; Logan, B.E.; Gorski, C.A.; Hall, D.M. An All-Aqueous Thermally Regenerative Ammonia Battery Chemistry Using Cu(I, II) Redox Reactions. *J. Electrochem. Soc.* **2021**, *168*, 070523. [CrossRef]
- Kratochvil, B.; Betty, K.R. A Secondary Battery Based on the Copper(II)-(I) and (I)-(0) Couples in Acetonitrile. *J. Electrochem. Soc.* **1974**, *121*, 851–854. [CrossRef]
- Porterfield, W.W.; Yoke, J.T. *Inorganic Compounds with Unusual Properties*; King, R.B., Ed.; ACS Publications: Washington, DC, USA, 1976; pp. 104–110.
- Peljo, P.; Lloyd, D.; Doan, N.; Majaneva, M.; Kontturi, K. Towards a thermally regenerative all-copper redox flow battery. *Phys. Chem. Chem. Phys.* **2014**, *16*, 2831–2835. [CrossRef] [PubMed]
- Lloyd, D.; Vainikka, T.; Kontturi, K. The development of an all copper hybrid redox flow battery using deep eutectic solvents. *Electrochim. Acta* **2013**, *100*, 18–23. [CrossRef]
- Sanz, L.; Palma, J.; García-Quismondo, E.; Anderson, M. The effect of chloride ion complexation on reversibility and redox potential of the Cu(II)/Cu(I) couple for use in redox flow batteries. *J. Power Sources* **2013**, *224*, 278–284. [CrossRef]
- Leung, P.; Palma, J.; Garcia-Quismondo, E.; Sanz, L.; Mohamed, M.R.; Anderson, M. Evaluation of electrode materials for all-copper hybrid flow batteries. *J. Power Sources* **2016**, *310*, 1–11. [CrossRef]
- Stricker, E.A.; Krueger, K.W.; Savinell, R.F.; Wainright, J.S. Investigating a Bromide Supported Electrolyte for an All-Copper Flow Battery. *J. Electrochem. Soc.* **2018**, *165*, A1797–A1804. [CrossRef]
- Bartolozzi, M. Development of redox flow batteries. A historical bibliography. *J. Power Sources* **1989**, *27*, 219–234. [CrossRef]
- Parasuraman, A.; Lim, T.M.; Menictas, C.; Skyllas-Kazacos, M. Review of material research and development for vanadium redox flow battery application. *Electrochim. Acta* **2013**, *101*, 27–40. [CrossRef]
- Sánchez-Díez, E.; Ventosa, E.; Guarnieri, M.; Trovò, A.; Flox, C.; Marcilla, R.; Soavi, F.; Mazur, P.; Aranzabe, E.; Ferret, R. Redox flow batteries: Status and perspective towards sustainable stationary energy storage. *J. Power Sources* **2021**, *481*, 228804. [CrossRef]
- Sharma, V.K.; Millero, F.J. Equilibrium Constants for the Formation of Cu(I) Halide Complexes. *J. Solut. Chem.* **1990**, *19*, 375–390. [CrossRef]
- Zhou, Q.; Zeng, D.; Voigt, W. Thermodynamic modeling of salt-water systems up to saturation concentrations based on solute speciation: CuCl₂-MCl_n-H₂O at 298 K (M = Li, Mg, Ca). *Fluid Phase Equilibria* **2012**, *322*, 30–40. [CrossRef]
- Applegarth, L.M.; Corbeil, C.R.; Mercer, D.J.W.; Pye, C.C.; Tremaine, P.R. Raman and ab Initio Investigation of Aqueous Cu(I) Chloride Complexes from 25 to 80 °C. *J. Phys. Chem. B* **2014**, *118*, 204–214. [CrossRef] [PubMed]
- Meng, Y.; Bard, A.J. Measurement of Temperature-Dependent Stability Constants of Cu(I) and Cu(II) Chloride Complexes by Voltammetry at a Pt Ultramicroelectrode. *Anal. Chem.* **2015**, *87*, 3498–3504. [CrossRef]
- Stricker, E.A.; Adler, Z.; Wainright, J.S.; Savinell, R.F. Diffusion Coefficients of Cuprous and Cupric Ions in Electrolytes with High Concentration of Bromide Ions. *J. Chem. Eng. Data* **2019**, *64*, 1095–1100. [CrossRef]
- Soltani, R.; Dincer, I.; Rosen, M.A. Kinetic and electrochemical analyses of a CuCl/HCl electrolyzer. *Int. J. Energy Res.* **2019**, *43*, 6890–6906. [CrossRef]
- Hall, M.; Akinfiev, N.N.; LaRow, E.G.; Schatz, R.S.; Lvov, S.N. Thermodynamics and Efficiency of a CuCl(aq)/HCl(aq) Electrolyzer. *Electrochim. Acta* **2014**, *143*, 70–82. [CrossRef]

29. Balashov, N.; Schatz, R.S.; Chalkova, E.; Akinfiev, N.N.; Fedkin, M.V.; Lvov, S.N. CuCl Electrolysis for Hydrogen Production in the Cu–Cl Thermochemical Cycle. *J. Electrochem. Soc.* **2011**, *158*, B266–B275. [[CrossRef](#)]
30. Sanz, L.; Lloyd, D.; Magdalena, E.; Palma, J.; Anderson, M.; Kontturi, K. Study and characterization of positive electrolytes for application in the aqueous all-copper redox flow battery. *J. Power Sources* **2015**, *278*, 175–182. [[CrossRef](#)]
31. Wu, Z.-C.; Awakura, Y.; Ando, S.; Majima, H. Determination of the Diffusion Coefficients of CuCl_2 , FeCl_3 , CuSO_4 , and $\text{Fe}_2(\text{SO}_4)_3$ in Aqueous Solutions. *Mater. Trans. JIM* **1990**, *31*, 1065–1071. [[CrossRef](#)]
32. Zhao, H.; Chang, J.; Boika, A.; Bard, A.J. Electrochemistry of High Concentration Copper Chloride Complexes. *Anal. Chem.* **2013**, *85*, 7696–7703. [[CrossRef](#)]
33. Saveant, J.-M. *Elements of Molecular and Biomolecular Electrochemistry*; John Wiley & Sons: Hoboken, NJ, USA, 2006.
34. Bard, A.J.; Faulkner, L.R. *Electrochemical Methods*, 2nd ed.; Wiley: New York, NY, USA, 2001.
35. Dai, Q.; Xu, J.J.; Li, H.J.; Yi, H.B. Ion association characteristics in MgCl_2 and CaCl_2 aqueous solutions: A density functional theory and molecular dynamics investigation. *Mol. Phys.* **2015**, *113*, 3545–3558. [[CrossRef](#)]
36. Wang, M.; Wang, C.; Cai, H.; Li, Y.; Zhang, Q.; Yi, H. Molecular dynamics simulation study on distinctive hydration characteristics of highly coordinated calcium chloride complexes. *J. Mol. Liq.* **2019**, *274*, 261–269. [[CrossRef](#)]
37. Kusmanov, S.A.; Silkin, S.A.; Belkin, P.N. Effect of Plasma-Electrolytic Polishing on the Corrosion Resistance of Structural Steels after Their Anodic Saturation with Nitrogen, Boron, and Carbon. *Russ. J. Electrochem.* **2020**, *56*, 356–364. [[CrossRef](#)]
38. Ngamchuea, K.; Eloul, S.; Tschulik, K.; Compton, R.G. Planar diffusion to macro disc electrodes—What electrode size is required for the Cottrell and Randles-Sevcik equations to apply quantitatively? *J. Solid State Electrochem.* **2014**, *18*, 3251–3257. [[CrossRef](#)]
39. Nikolenko, M.V.; Vasylenko, K.V.; Myrhorodska, V.D.; Kostyniuk, A.; Likozar, B. Synthesis of Calcium Orthophosphates by Chemical Precipitation in Aqueous Solutions: The Effect of the Acidity, Ca/P Molar Ratio, and Temperature on the Phase Composition and Solubility of Precipitates. *Processes* **2020**, *8*, 1009. [[CrossRef](#)]
40. Zhang, N.; Zhou, Q.; Yin, X.; Zeng, D. Trace Amounts of Aqueous Copper(II) Chloride Complexes in Hypersaline Solutions: Spectrophotometric and Thermodynamic Studies. *J. Solut. Chem.* **2014**, *43*, 326–339. [[CrossRef](#)]
41. Zhang, N.; Tang, J.; Ma, Y.; Liang, M.; Zeng, D.; Heftet, G. A spectroscopic study of solvent effects on the formation of $\text{Cu}(\text{II})$ -chloride complexes in aqueous solution. *Phys. Chem. Chem. Phys.* **2021**, *23*, 6807. [[CrossRef](#)]
42. Manahan, S.E.; Iwamoto, R.T. Chloro Complexes of Copper(II) and Copper(I) in Acetonitrile. *Inorg. Chem.* **1965**, *4*, 1409–1413. [[CrossRef](#)]
43. Miessler, G.; Tarr, D. Inorganic Chemistry. In *Pearson Educational International*, 3rd ed.; Prentice Hall, 2011; pp. 367–369. Available online: <https://hostnezt.com/cssfiles/chemistry/Inorganic%20Chemistry%20By%20GARY%20L.%20MIESSLER.pdf> (accessed on 30 November 2021).
44. Mereshchenko, A.; Olshin, P.K.; Myasnikova, O.S.; Panov, M.; Kochemirovsky, V.; Skripkin, M.; Moroz, P.; Zamkov, M.; Tarnovsky, A. Ultrafast Photochemistry of Copper(II) Monochlorocomplexes in Methanol and Acetonitrile by Broadband Deep-UV-to-Near-IR Femtosecond Transient Absorption Spectroscopy. *J. Phys. Chem. A* **2016**, *120*, 1833–1844. [[CrossRef](#)]